PETROLOGY OF THE UNBRECCIATED EUCRITE, CUMULUS HILLS 04049 Jasmeet K. Dhaliwal[1], Christopher A. Corder[1], James M.D. Day[1], Allan D. Patchen[2], Lawrence A. Taylor[2], [1]Scripps Institution of Oceanography, UCSD, 9500 Gilman Dr., La Jolla, CA 92093, USA (correspondence: jasmeetd@ucsd.edu), [2]Planetary Geosciences Institute, Dept. of Earth & Planetary Sciences, University of Tennessee, Knoxville, Tennessee, 37996.

Introduction: Eucrite meteorites represent early-formed (~4.557-4.565 Ga) crustal basalts and basaltic to gabbroic cumulates from the howardite-eucrite-diogenite (HED) parent body or bodies (e.g., [1]). The HED are commonly thought to originate from the asteroid Vesta (e.g., [2-3]), although O-isotopes for eucrites [4] and diogenites [5] indicate more than one parent body. Approximately 85% of eucrites in the terrestrial collections are polymict to monomict breccias, with the remainder of eucrites being unbrecciated. The unbrecciated eucrites are important for understanding lithological diversity on their parent body(ies), which is especially relevant with the ongoing DAWN mission to Vesta [1]. Unbrecciated eucrites are also important for understanding early planet differentiation mechanisms, where unbrecciated eucrites may be free from the influence of post-crystallization impact additions. Here we present the petrology and mineral chemistry of eucrite Cumulus Hills (CMS) 04049.

Methods: Petrography and mapping of the section CMS 04049, 27 was performed using a petrographic microscope. Regions of interest were further imaged and quantitative major mineral compositions were analyzed using a Cameca SX-100 electron microprobe at the University of Tennessee.

Mineral chemistry: CMS 04049 is a monomict unbrecciated eucrite with a predominantly sub-ophitic texture (Figure 1) with 35:65 plagioclase to pyroxene, and lesser amounts of silica, ilmenite, chromite and troilite with minor zircon and olivine, broadly consistent with previous observations [6-7].

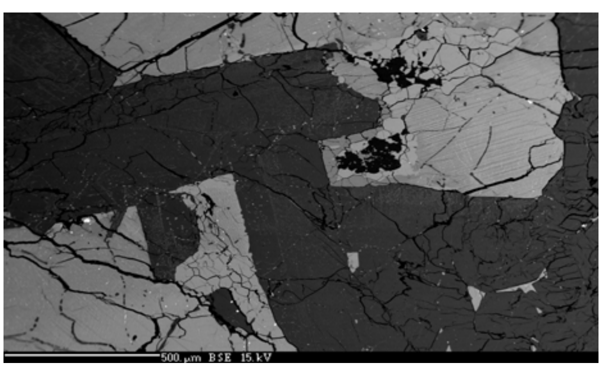

Figure 1: *Back-scatter electron (BSE) image of CMS 04049, 27 showing the sub-ophitic texture of plagioclase (dark gray) and pyroxene (light gray) and granoblastic regions with high Fe-pyroxene and silica (note 500 µm scale bar).*

The section contains a relatively high abundance of oxide minerals and FeS (0.7 modal %). Exsolution lamellae occur in high-Ca pyroxenes (Figure 1) and some pyroxenes exhibit a 'herringbone texture', also seen in Yamato 791186 [8]. Pyroxenes range from high-Ca ($En_{27}Wo_{40}$) to low-Ca, high-Fe compositions ($En_{40}Wo_{3}$) (Figure 2). Intermediate ($En_{35}Wo_{15}$ to $En_{32}Wo_{32}$) pyroxenes occur as exsolution lamellae and are likely an artifact of mixing between the high-Ca and low-Ca, high-Fe pyroxene compositions. The pyroxene compositions are consistent with other unbrecciated sub-ophitic eucrites [1] and suggest that CMS 04049 is equilibrated. On the basis of major element pyroxene composition [8], CMS 04049 is type 6, or slowly cooled.

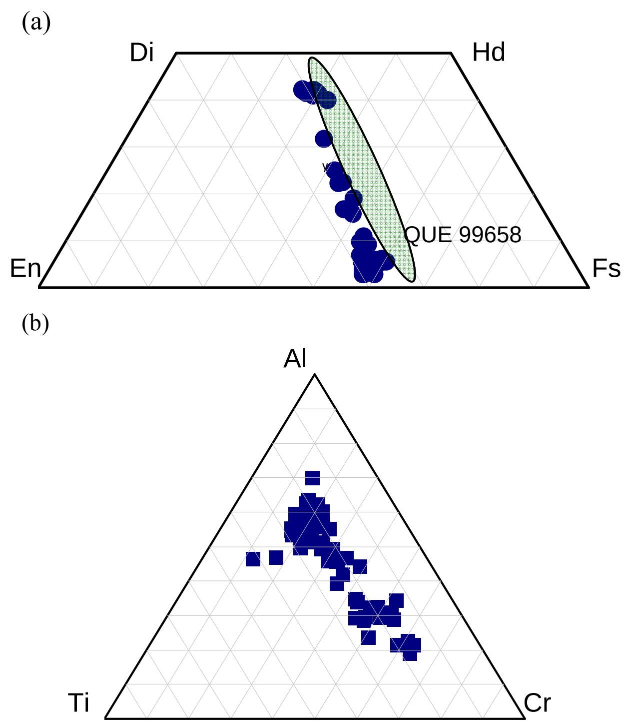

Figure 2*: (a) Compositions of CMS 04049 (blue) pyroxenes with field of pyroxene compositions from QUE 99658 [1] sub-ophitic unbrecciated eucrite shown for comparison. (b) Minor (Al, Cr, and Ti) element compositions for CMS 04049 (blue) pyroxene.*

Plagioclase compositions range from An_{86-98}. Spinels have homogeneous compositions (Cr/(Cr+Al) × 100 = 81.5 ±0.7) and are found as individual grains or associated with large ilmenites. Fayalitic olivine (Fo_{26}) is found associated with Cr-spinel. Sulphides in the sample consist entirely of troilite, with low nickel (0.01 ±0.01 wt.%; 2 S.D.) and cobalt (0.03 ± 0.02 wt.%; 2 S.D.). One metal grain (5 µm) and two zircon grains (10-15 µm) were found in the sample but were not quantitatively analyzed.

Texture: CMS 04049, 27 exhibits three textures: (1) a primary relatively coarse-grained (>1 mm) sub-ophitic and highly shocked texture similar to Chervony Kut or EET 92004 (e.g., [1]) (Figure 1); (2) lesser regions with a granoblastic texture composed predominantly of pyroxene and silica (Figure 1); (3) a large (6 mm by 4 mm) and conspicuously unequilibrated region dominated by high-reflectivity Fe-sulphides and spinels (Figure 3). Shock effects are also evident in our sample, in the form of visible darkening of pyroxenes.

Figure 3: The large mesostasis region (outlined) in CMS 04049, 27 under reflected light. Note the large high reflectively ilmenite grains and sulphides, making 0.7 modal %.

Mineral compositional variations correspond broadly with textural regions. For example, all measured silica grains occur in granoblastic regions. It is notable that the olivine measured in CMS 04049 is within the primary sub-ophitic texture, associated with Cr-spinel, whereas previously reported olivine typically occurs in mesostasis regions in unbrecciated eucrites [1]. Fe-rich pyroxenes are more concentrated within the mesostasis regions, while exsolved pyroxenes occur in primary sub-ophitic regions (Figure 4). With the exception of a few measured grains, the ilmenite occurs in mesostasis regions while the Cr-spinel is located within mostly primary and some granoblastic regions.

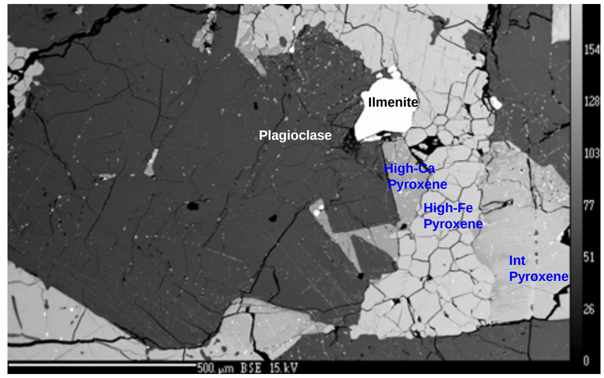

Figure 4: BSE image of CMS 04049, 27 showing a region of exsolved pyroxene with intermediate composition occurring alongside a large sub-rounded ilmenite grain (note 500 µm scale bar).

Discussion: While CMS 04049 shares many similarities with unbrecciated subophitic and relatively slowly-cooled eucrites, such as Chevrony Kut, EET 92004, PCA 91078, PCA 82501, or QUE 99658 [1], CMS 04049 has a younger crystallization age (4558.4 ±0.6 Ma [7]) than Chevrony Kut (~4564 Ma [7]). CMS 04049, 27 differs from other subophitic eucrites in that it is also dominated by a large mesostasis region with high sulphide content. Mesostasis regions of this size are an uncommon feature of most unbrecciated eucrites [1] and it has been argued that there should be no primary mesostasis in slowly cooled (i.e., Type 6 [8]) eucrites. Given the crystallization age of CMS 04049 that suggests a protracted thermal history, we envisage two possible explanations for the extensive mesostasis in CMS 04049, 27. In the first instance, the mesostasis areas are in fact primary, with textures reflecting immiscibility and slow-cooling. Alternatively, the mesostasis regions represent secondary melting processes resulting from thermal metamorphism during impact [8]. Further work is on-going to distinguish between these possibilities.

Acknowledgements: We thank the Meteorite Working Group for loan of sample CMS 04049, 27 and acknowledge the NASA Cosmochemistry Program (NNX12AH75G) for support.

References: [1] Mayne, R.G. et al. (2009) *GCA,* **73**, 794-819. [2] McCord T.B. et al. (1970) *Science,* **168**, 1445-1447. [3] Binzel R.P. & Xu S. (1993) *Science,* **260**, 186-191. [4] Scott E.R.D. et al. (2009) *GCA,* **73**, 5835-5853. [5] Day J.M.D. et al. (2012) *Nat. Geosci.* **5**, 614-617 [6] Righter M. & Lapen T.J. (2010) *LPSC XLI,* Abstract #2629. [7] Shukolyukov A. & Lugmair G.W. (2008) *LPSC XXXIX,* Abstract #2094. [8] Takeda, H. & Graham, A. L. (1991), *Meteoritics, 26* 129-134.